Mechanical behaviour of isotactic polypropylene subjected to various strain histories in uniaxial extension

J. M. Crissman and L. J. Zapas
Center for Materials Science, National Bureau of Standards, Washington, D.C. 20234, USA
(*Received* 3 *May* 1982)

The mechanical behaviour of a slowly quenched isotactic polypropylene has been studied for various strain histories in extension. Creep, constant rate of strain, and constant rate of loading experiments were carried out at deformations up to and beyond the point where necking occurs. A creep diagram, which includes the failure envelope, is presented. From the available data we have also obtained an extrapolated surface of the single step stress–relaxation behaviour. From this surface we can calculate, using the Bernstein and Zapas theory on the instability of viscoelastic bars, the deformation at which necking occurs for various strain histories.

Keywords Creep; instability theory; mechanical behaviour; polypropylene; stress relaxation

INTRODUCTION

In 1975 Ericksen[1] presented work on the discontinuous deformations of solid elastic bars. Recently Bernstein and Zapas[2] extended this work to viscoelastic materials which obey the BKZ theory[3]. As in the case of Ericksen's work, the Bernstein and Zapas treatment cannot predict *a priori* when the material will exhibit the phenomenon of necking, but it does give an explanation for the formation of the neck, which depends on the stretch history. Here, (1) we present experimental data, obtained using a variety of strain histories, for a material which can be described fairly well by the BKZ theory, and (2) we show consistency between the theory and the experimental results by suitably extrapolating the available data into regions which are not accessible experimentally.

For this purpose, we have selected as a material for our experiments a rather slowly quenched isotactic polypropylene. A set of experiments was performed which involved a variety of different strain histories in uniaxial extension. These included single step stress–relaxation, constant rate of strain, constant rate of loading, and creep under a fixed applied load. In each case the measurements were made up to and beyond the point of necking until fracture occurred.

THEORETICAL CONSIDERATIONS

We shall be concerned only with deformation histories in uniaxial extension, and begin by considering a bar of material which has been at rest at all times up to $\tau=0$; its length in the undeformed state is l_0. At time $\tau\geqslant 0$ it is subjected to a given stretch history, whereby the bar at time τ has a length $l(\tau)$. In this situation the BKZ theory[3] gives the following relationship:

$$\hat{\sigma}(t)=H(\mu(t),t)-\int_0^t H_*\left(\frac{\mu(t)}{\mu(\tau)},t-\tau\right)\mathrm{d}\tau, \qquad (1)$$

where $\hat{\sigma}(t)$ is the true stress at time t, and $\mu(\tau)=l(\tau)/l_0$. Throughout this paper we shall follow the convention that prime means the derivative of the function with respect to the first argument, and star means the derivative with respect to the second argument. Thus:

$$H'(\mu,t)=\frac{\partial H(\mu,t)}{\partial\mu(\tau)}, \text{ and } H_*(\mu,t)=\frac{\partial H(\mu,t)}{\partial t}.$$

From equation (1), it can be seen that if the bar at time $\tau=0$ is subjected to a single step in strain, $\mu(t)$, then the stress necessary to keep the bar stretched at time t is equal to $H(\mu(t),t)$, where $H(1,t)=0$. From data obtained from single step stress–relaxation experiments carried out at different levels of strain, it is evident that one can determine the stress response for any other strain history in uniaxial extension. However, since equation (1) is nonlinear, one cannot determine the strain as a function of the stress, as for example in a creep experiment. Equation (1) applies to the type of experiment where knowing the strain history one can determine the stress response and the calculated values can then be compared with experimentally determined quantities.

Bernstein and Zapas[2] have shown that for certain materials, which we shall refer to as BKZ materials, an instability may occur at some level of strain, the result of which is the phenomenon of necking. In order to be consistent with their nomenclature, we shall rewrite equation (1) in the form:

$$\sigma(t)=w'(\mu(t),t)-\int_0^t \frac{1}{\mu(\tau)}w'_*\left(\frac{\lambda}{\mu(\tau)},t-\tau\right)\mathrm{d}\tau, \qquad (2)$$

where $\sigma(t)$ now is the engineering stress and:

$$w'(\mu(t),t)=\frac{1}{\mu(t)}H(\mu(t),t)$$

0032—3861/83/030351–08$03.00

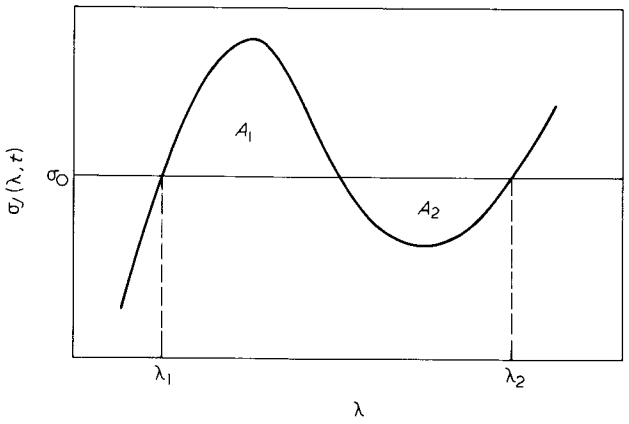

Figure 1 Isochronal jump curve

Bernstein and Zapas then define a jump stress as follows:

$$\sigma_J(\lambda,t)=w'(\lambda,t)-\int_0^t \frac{1}{\mu(\tau)}w'_*\left(\frac{\lambda}{\mu(\tau)},t-\tau\right)\mathrm{d}\tau \qquad (3)$$

In equation (3), $\sigma_J(\lambda,t)$ is the value of the instantaneous stress that the material would produce at time $\tau=t$ upon being subjected to an instantaneous stretch of magnitude λ following a history $\mu(\tau)$. For a particular history, $\mu(\tau)$, one can obtain the value of $\sigma_J(\lambda,\tau)$ for different values of λ. If the isochronal jump curve can be represented schematically as in *Figure 1*, then for the case where the area A_1 is larger than A_2 the material is stable, but when A_1 becomes smaller than A_2 necking will occur.

EXPERIMENTAL

Material and specimen preparation

The polymer was an experimental sample of isotactic polypropylene provided by the Avisun Corporation.* It had a viscosity average molecular weight of 207 000 and contained 2.56% material extractable in C_7H_{16}. It contained 0.02 per cent of stabilizer. This was the same material as that used in the earlier mechanical behaviour studies by Passaglia and Martin[4] and by Crissman[5].

As supplied, the material was in the form of pellets which initially were compression moulded into flat sheets having a nominal thickness of about 0.06 cm. This was accomplished by placing the pellets in a mould which consisted of two chromed photographic plates separated by a 0.06 cm thick aluminium plate having a 15 cm diameter hole. The mould was placed in a press and heated to 463 K (~190°C) at which temperature it was held for ten min. Pressure sufficient to ensure the proper fusion of the moulded polymer was then applied, after which the entire mould was quickly removed from the press and plunged into cold water.* Sheets prepared in this manner had a density ranging from 0.898 to 0.901 g cm^{-3}. Specimens having one of two types of geometries were cut from the sheets with a die. For the single step stress–relaxation experiments the specimens were cut to conform with the geometry of the 'T-50' bar described in ASTM D599-61 (ref. 6). In that geometry the width of the narrow section is constant over the entire portion of the specimen lying between the grips. For all of the other experiments the specimens conformed to the more conventional dumbbell geometry described in ASTM D638-72, type IV,[7] except that in the present case all the specimen dimensions were scaled down by a factor of two. The specimens were aged at room temperature for a period of at least one month prior to the experiments.

* Certain commercial materials and equipment are identified in this paper in order to specify adequately the experimental procedure. In no case does such identification imply recommendation or endorsement by the National Bureau of Standards, nor does it imply necessarily the best available for the purpose.

Apparatus and method

Creep experiments were done at room temperature (297 ± 0.5 K) under conditions of dead loading (constant applied engineering stress) in the range from 14.2 to 23.2 MPa. The elongation of the specimen as a function of time was determined by monitoring with a cathetometer the distance between fiducial marks placed on the guage section of the dumbbell.

Single step stress–relaxation experiments were carried out at 297 K in an environmental chamber in which the temperature held constant to within 0.03 K over the duration of the test. A correction to the stress–relaxation data has been made which concerns the fact that a finite time is required in order to apply the step in strain. Zapas and Phillips[8] have shown that to a good approximation the relaxation function can be represented by the relation:

$$\sigma(t+t_1/2)/\varepsilon$$

where t is the time following application of the step, t_1 is the time required to impose the step, and ε is the strain. In the present set of experiments the step time was generally in the range from 0.5 to 1.5 s, so that in our data the correction rapidly becomes small.

Two other types of experiments will be described in this work. These are histories involving constant rate of clamp separation and constant rate of loading (engineering stress). Both experiments were done on a servo-controlled hydraulic test machine. Because of the large deformations to which these specimens were subjected, the strain was determined with the aid of a cathetomer rather than an extensometer.

RESULTS

Single step stress–relaxation

A knowledge of the single step stress–relaxation behaviour (at various strains and times) in uniaxial extension is sufficient to describe the behaviour for any other strain history in uniaxial extension, at least within the range of strains and times for which the experimental data are available. In such an experiment the specimen, at a time $t=0$, is subjected to a sudden step in strain and the stress response is measured as a function of time. In the present work we have examined the stress–relaxation behaviour for a series of steps in strain up to 9.0%, and some of the data are tabulated in *Table 1*. At strains greater than about 9–10% the specimens always necked upon application of the step.

In *Figure 2*, the data in *Table 1* have been replotted as isochrones of log true stress *versus* log strain. The isochrones cover four decades in time. The behaviour is highly nonlinear over nearly the entire range of strains

Table 1 Stress–relaxation data for slowly quenched isotatic polypropylene

Time (s)	True stress (MPa) for the values of strain indicated				
	$\epsilon = 0.0037$	$\epsilon = 0.0079$	$\epsilon = 0.0126$	$\epsilon = 0.0288$	$\epsilon = 0.076$
0.62	5.37	11.1	17.0	27.4	36.8
1.25	5.33	11.0	16.7	26.2	33.0
1.88	5.26	10.9	16.4	25.2	30.9
3.13	5.18	10.7	16.0	24.3	29.1
4.40	5.14	10.5	15.7	23.6	28.2
9.40	5.01	10.2	14.9	22.2	26.4
14.4	4.90	10.0	14.5	21.4	25.2
29.4	4.76	9.60	13.8	20.3	23.8
59.4	4.61	9.30	13.1	19.0	22.4
120	4.44	8.90	12.3	18.1	21.1
240	4.30	8.50	11.6	17.0	20.0
480	4.16	8.20	11.0	16.1	18.9
1000	3.99	7.80	10.3	15.1	17.9
2000	3.88	7.50	9.60	14.2	17.0
3600	3.76	7.11	9.10	13.6	16.3
7200	3.62	6.87	8.70	12.8	15.5
10000	3.57	6.75	8.40	12.6	14.8

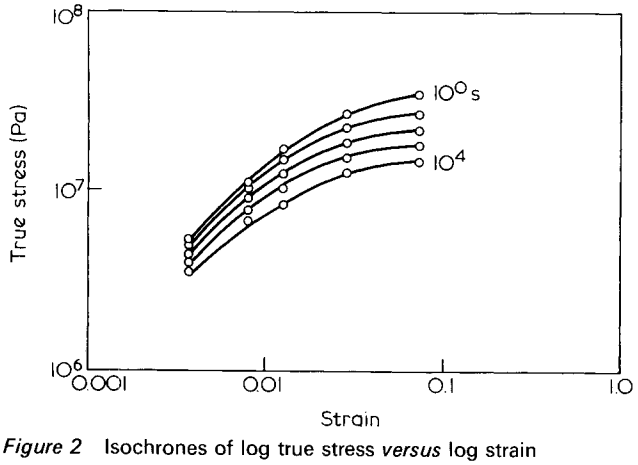

Figure 2 Isochrones of log true stress *versus* log strain

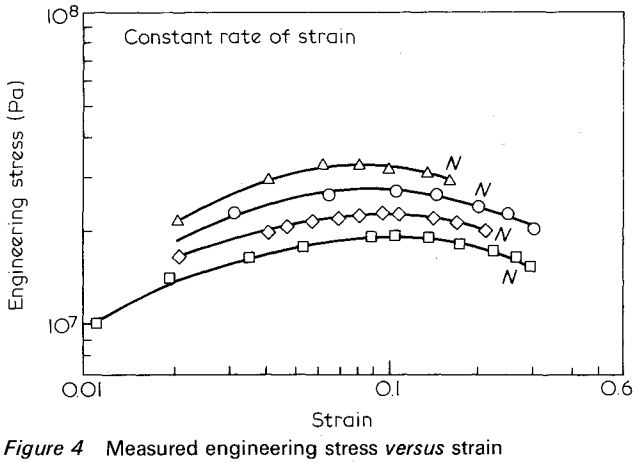

Figure 4 Measured engineering stress *versus* strain

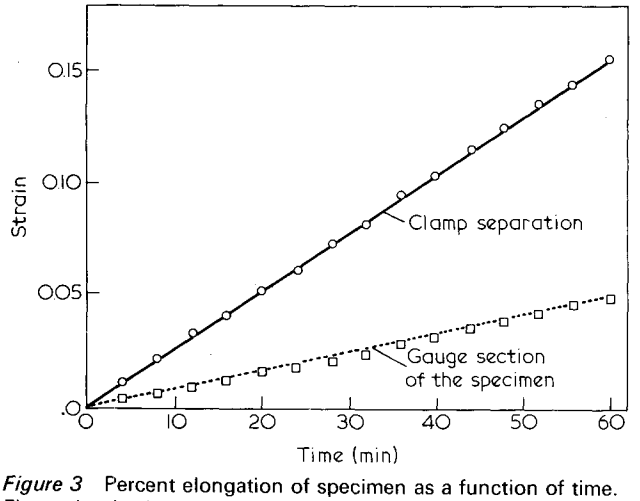

Figure 3 Percent elongation of specimen as a function of time. Elongation is also shown in absence of end effects

examined. For the polypropylene the stress–strain behaviour becomes linear only in the region of strain below 1%. Observe that at a strain of 7.6% the isochrones are flattening to a zero slope, and the modulus has been reduced by a factor of at least 3.2 from what it would have been if the behaviour were linear. Also, at strains above about 3% the nonlinearity becomes essentially independent of time, i.e. the isochrones form a set of nearly parallel curves.

Constant rate of strain experiments

In this set of experiments the specimens were extended at a constant rate of clamp separation. In *Figure 3*, we show for one experiment (at a rate of 5×10^{-5}) the per cent elongation of the specimen, as measured between fiducial marks placed on the guage portion of the dumbbell, as a function of time. Also shown is the elongation which the specimen would have had in the absence of end effects. The dotted straight line drawn through the point (0,0) does not deviate much from the actual data points, therefore, we can assume that the experiments were done at constant rate of elongation. In *Figure 4* the measured engineering stress *versus* strain is shown for four different rates which vary by a factor of 10^3. The first result of interest is that the stress (for a given strain) varies only by a factor of 1.7 even though the rate varied by a factor 10^3. Also, the specimens did not neck at the strain, ε_M (the strain at the maximum stress), but necked at a larger strain, ε_N, as is indicated by the letter N in *Figure 4*. The maximum in the stress, σ_M, and the strain at the point of necking, ε_N, both occur at successively larger strains as the rate of elongation decreases. After necking occurred the

Table 2 Summary of constant rate of strain experiments

κ^a	$\sigma_M{}^b$	$\epsilon_M{}^c$	$\epsilon_N{}^d$	$\sigma_P{}^e$
6.8×10^{-3}	29.6	0.08	0.16	19.2
6.0×10^{-4}	27.0	0.10	0.19	17.4
5.1×10^{-5}	22.9	0.10	0.21	14.8
7.6×10^{-6}	19.2	0.12	0.24	12.8

[a] Rate of strain per second
[b] Maximum stress prior to necking (MPa)
[c] Strain at the point of maximum stress
[d] Strain at the point where necking occurred
[e] Plateau value of stress (MPa)

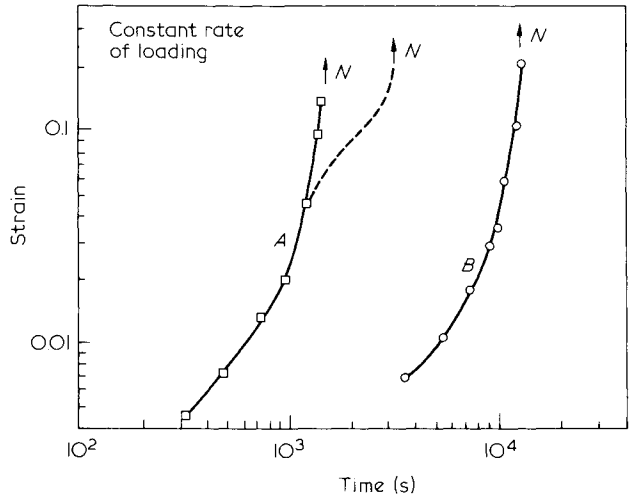

Figure 5 Log strain *versus* log time

stress plateaued before rising again at the very large strains. Values of ϵ_M, σ_M, ϵ_N, and σ_P as a function of the rate κ are summarized in *Table 2*.

Using equation (1), we have calculated the stress for a constant rate of elongation experiment, and the values obtained were somewhat lower than the experimental values, the maximum deviation being about 7%. The existence of the maximum in the engineering stress suggests that $w'(\mu,t)$, at constant μ, has a maximu, and the position of the various maxima will depend upon time. The isochrones at the shorter times will have a maximum at smaller values of strain.

Constant rate of loading

This experiment involves increasing the engineering stress at a constant rate and the strain is determined as a function of time. One characteristic of constant rate of loading experiments is that as soon as the specimen has necked it breaks. *Figure 5* shows log strain *versus* log time for specimens subjected to rates of loading which differed by a factor of ten. The curves A and B can be superposed by a shift along the time axis alone. At a rate of 1.83×10^{-3} the specimen necked and broke at a strain of about 0.14, whereas at a rate of 1.78×10^{-4} fracture occurred at a strain of 0.22. As in the constant rate of strain experiment, necking occurred at a higher strain in the specimen subjected to the lower rate of loading. Since the two curves A and B can be superposed, it can be shown from the BKZ theory that σ *versus* ε can also be superposed by a shift along the stress axis. That this is true can be seen in *Figure 6* where we have shown a plot of log stress *versus* log strain for the same two rates of loading. We note that for the constant rate of loading experiments the strain was determined with the aid of a cathetometer rather than an extensometer in order to avoid the possibility that the attachment of the extensometer could contribute to the premature necking of the specimen.

In a third constant rate of loading experiment, shown by the dashed line in *Figure 5*, the data were obtained using two different rates of loading. The initial rate was the same as that for the specimen subjected to a rate of 1.83×10^{-3}. Then when a stress of 2.20×10^7 Pa was reached the rate was changed to a much slower one ($\simeq 1.8 \times 10^{-5}$), so that the stress response was nearly constant, and the second step could almost be considered as a creep experiment. For this specimen, necking and fracture occurred at a strain of 0.19, which was intermediate to the strains at which the other two specimens broke.

Creep

Shown in *Figure 7* are creep curves for eight specimens subjected to engineering stresses in the range 14.2–23.2 MPa. The letter *N* indicates the time and strain at which the specimens necked and the letter β the elongation at which the neck had propagated through the straight portion of the specimen. Except for the specimen having

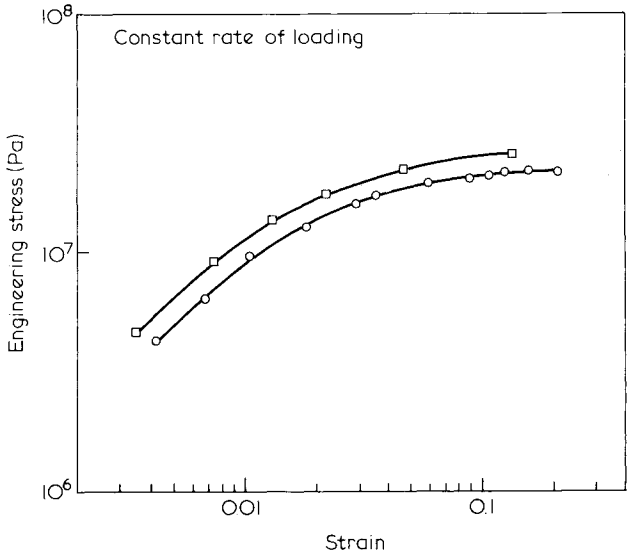

Figure 6 Plot of log stress *versus* log strain

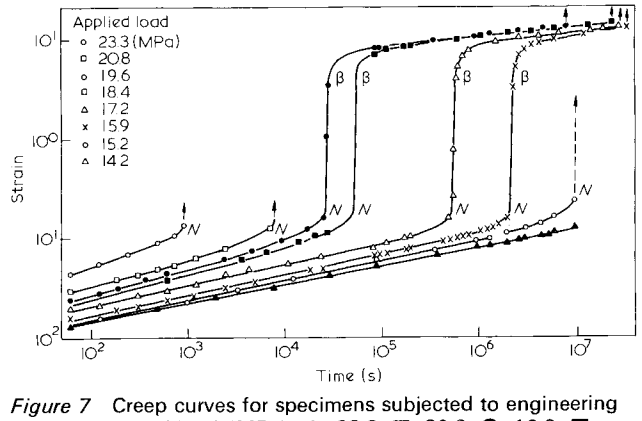

Figure 7 Creep curves for specimens subjected to engineering stresses: Applied load (MPa): ○; 23.3; □, 20.8; ●, 19.6; ■, 18.4; △, 17.2; ×, 15.9; ○, 15.2; ▲, 14.2

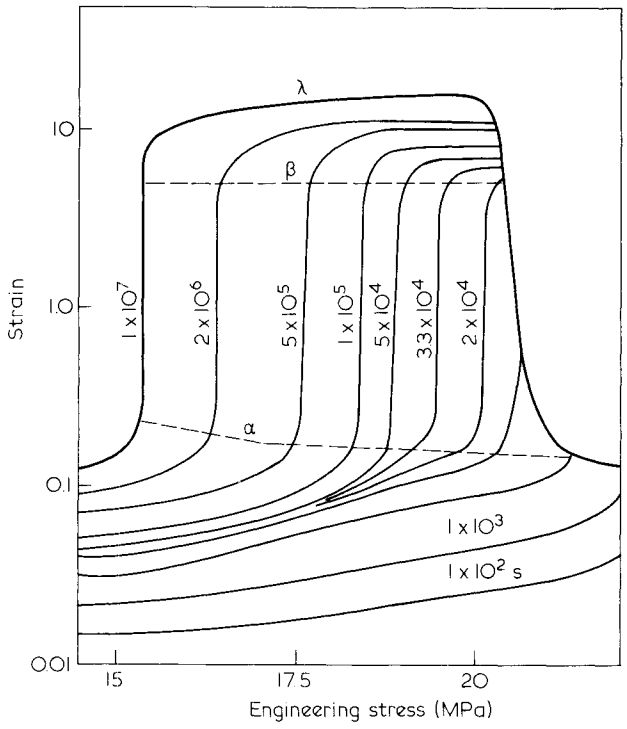

Figure 8 Data from *Figure 8* in terms of isochrones of strain *versus* the applied engineering stress

the smallest load (filled triangles) the creep experiment was continued up until the point at which fracture occurred. The two specimens having the largest loads (open circles and squares) both fractured almost immediately upon necking. The four specimens having intermediate loads all drew substantially before fracture occurred. For these four the maximum stretch (λ) was 14–15, which means that the point β ($\lambda = 6$) represents only about 40% of the total creep attainable in this material at room temperature. The specimen under stress of 15.2 MPa (hexagons) necked and then fractured during the early stages of drawing. Even though this specimen required much longer to neck than did three of the specimens having higher loads, it is interesting that it fractured sooner. A general observation is that the point at which necking occurred shifts to larger strain with decreased load.

As an aside we note that the creep behaviour of the polypropylene is in many respects similar to that of linear polyethylenes which have a weight average molecular weight in the range from 0.9×10^5 to 2.0×10^5, and a number average molecular weight of $\sim 1.5 \times 10^4$. We have shown in previous work[9] that in uniaxial creep polyethylene exhibits at least two distinct failure modes. In one case, that of relatively large stresses, the material undergoes an instability which leads to necking, and then, depending upon the molecular weight and molecular weight distribution, may cold-draw substantially before breaking. In the second case, that of relatively small stresses, the specimen no longer exhibits necking, but rather fails by cracking. In the latter case the fracture can occur at strains as small as 5% and below. In the case of polyethylene, the transition from a mechanism of necking and cold-drawing to one of cracking occurs over the range of stresses from about 13.5 to 16.5 MPa, and at times near 10^5 s. We have observed that in the transition region a specimen may exhibit both necking and cracking at the same time, and in this region it becomes difficult to predict just which mechanism will ultimately cause the failure.

If the same two failure modes occur in the case of polypropylene, then it is clear from *Figure 7* that the mechanism of cracking does not appear until times of nearly 10^7 are reached. For example, in the specimen loaded to a stress of 15.2 MPa numerous small cracks and/or crazes appeared beginning at a strain of 12–14%, and these may have contributed to its apparent early fracture. It is also true that the specimen stressed at 14.2 MPa (filled triangles) began exhibiting small cracks and/or crazes at a strain of $\sim 10\%$. It is possible that this specimen would have failed by cracking had the experiment been continued, but it may have required up to one to two years londer under load. In this regard we have observed that for an ethylene–hexene copolymer which was lightly branched, having one to two butyl side groups per one thousand carbon atoms, a time of nearly three years was required at room temperature for the failure mode to switch from one of necking and cold drawing to one of crack growth.

Following a procedure which we developed previously[9,10], the creep data in *Figure 7* have been replotted in *Figure 8* in terms of isochrones of strain *versus* the applied engineering stress. Because of the high values of strain which this material achieves in the fully drawn state, the data are plotted semilogarithmically. We distinguish three regions bounded by the lines α, β and γ. Below line α is the region in which the material deforms homogeneously, and upon reaching line α necking occurs. Between the lines α and β lies a region in which both necked and unnecked material coexist. Above line β is a third region where now the drawn material deforms more or less homogeneously. Line γ represents the envelope for fracture. One can consider *Figure 8* to be a phase diagram for creep, where in the region between α and β two phases are present, one drawn material and the other undrawn material.

DISCUSSION

We stated earlier that, within the range of strains and times covered in our experiments, the stresses in a constant rate of strain experiment calculated using the BKZ theory were in good agreement with the experimental data. In all cases the calculated values were lower than the observed values, but the maximum deviation was 7% or less. This rather good agreement encouraged us to examine more closely the model proposed by Bernstein and Zapas concerned with the stability and cold-drawing of viscoelastic bars.

According to Bernstein and Zapas, for a material which has been subjected to a strain history $\mu(\tau)$, where $-\infty < \tau \leqslant t$, a stability criterion can be determined at time t, for which $\mu(\tau) = \mu(t)$, if the jump curve given by equation (3) can be determined. For the condition $\lambda = \mu(t)$, equation (3) gives the stress response predicted by the BKZ theory, following a strain history $\mu(\tau)$. For convenience we shall rewrite equation (3) in the following form:

$$\sigma_J(\lambda,t) = w'(\lambda,t) - \int_0^t \frac{1}{\mu(t-\xi)} w'_* \left(\frac{\lambda}{\mu(t-\xi)}, \xi \right) d\xi \qquad (4)$$

where we have made the substitution $\tau = t - \xi$. When ξ

approaches zero, the ratio $\mu(t)/\mu(t-\xi)$ approaches unity and $w'_*(\mu(t)/\mu(t-\xi),\xi)$ goes to zero. However in the case of the jump curve, $\lambda/\mu(t-\xi)$ approaches the value $\lambda/\mu(t)$, which means that in the calculation of the integral, even values at $\xi=0$ contribute highly. Therefore we shall need to know the values of $w'(\lambda,t)$ at very short times, i.e. values corresponding to the material in the 'glassy state'. From the work of Passaglia and Martin[4] we estimated the value of the modulus corresponding to the glassy state to be about 4.1×10^9 Pa, assuming the Poisson ratio to be 0.4. From dynamic measurements in flexure carried out at room temperature and at frequencies from 150 to 2500 Hz it was found that the flexure modulus was constant to within one per cent and equal to about 1.62×10^9 Pa. Since this value is significantly lower than the modulus corresponding to the glassy state, and is constant over the frequency range examined, we assume that there exists a transition region as shown schematically in *Figure 9*. Then between the time t_1 and 1 s there is a plateau region. From the dynamic data we know that t_1 must be less than about 10^{-4} s. We then rewrite equation (4) in the form:

$$\sigma_J(\lambda,t)=w'(\lambda mt)-\int_0^{t_1}\frac{1}{\mu(t-\xi)}w'_*\left(\frac{\lambda}{\mu(t-\xi)},\xi\right)d\xi-\int_{t_1}^{t}\frac{1}{\mu(t-\xi)}w'_*\left(\frac{\lambda}{\mu(t-\xi)},\xi\right)d\xi \tag{5}$$

Since our interest is in experiments in which t is taken to be a long time compared to 0.1 s, for $\xi<0.1$ s $\mu(t-\xi)\cong\mu(t)$. Moreover, knowing that t_1 is much smaller than 0.1 s, the first integral in equation (5) can be written as:

$$-\int_0^{t_1}\frac{1}{\mu(t)}w'_*\left(\frac{\lambda}{\mu(t)},\xi\right)d\xi=\frac{1}{\mu(t)}\left\{w'\left(\frac{\lambda}{\mu(t)},0\right)-w'\left(\frac{\lambda}{\mu(t)},t_1\right)\right\} \tag{6}$$

But as a consequence of the existence of the plateau region discussed earlier, it follows that in the region from $t_1\leqslant t\leqslant1$:

$$w'\left(\frac{\lambda}{\mu(t)},t_1\right)=w'\left(\frac{\lambda}{\mu(t)},1\right)$$

thus the right hand side of equation 6 becomes:

$$\frac{1}{\mu(t)}\left\{w'\left(\frac{\lambda}{\mu(t)},0\right)-w'\left(\frac{\lambda}{\mu(t)},1\right)\right\} \tag{7}$$

As a result of equation (7), the integral in equation (6) depends only upon the values at the two limits and it is not necessary to know the values of the function w'_* in the transition zone.

Now the second integral in equation (5) can be rewritten as:

$$-\int_{t_1}^{t}\frac{1}{\mu(t-\xi)}w'_*\left(\frac{\lambda}{\mu(t-\xi)},\xi\right)d\xi=-\int_{\ln t_1}^{\ln t}\frac{1}{\mu(t-\xi)}w'\left(\frac{\lambda}{\mu(t-\xi)},\xi\right)\frac{\partial\ln w'}{\partial\ln\xi}d\ln\xi \tag{8}$$

But in the interval from t_1 to 1 s we have the relation:

$$\frac{\partial\ln w'}{\partial\ln\xi}=0$$

so that the right hand side of equation (8) becomes:

$$\int_0^{\ln t}\frac{\eta_s}{\mu(t-\xi)}w'\left(\frac{\lambda}{\mu(t-\xi)},\xi\right)d\ln\xi \tag{9}$$

where

$$\eta_s=-\frac{\partial\ln w'}{\partial\ln\xi}$$

A double logarithamic plot of the single step stress–relaxation data shows that at the higher levels of strain, the data, to a good approximation form a set of parallel straight lines. Therefore we shall assume that for times greater than one second η_s is a constant, independent of the strain. Then there exists a value $\xi=\xi_1$ such that:

$$-\int_0^{\ln t}\frac{\eta_s}{\mu(t-\xi)}w'\left(\frac{\lambda}{\mu(t-\xi)},\xi\right)d\ln\xi=\frac{\eta_s}{\mu(t-\xi_1)}w'\left(\frac{\lambda}{\mu(t-\xi_1)},\xi_1\right)\ln t \tag{10}$$

In the calculations for the constant rate of strain the value $\xi_1=\sqrt{t}$ gave good agreement with the graphical integration of the right hand side of equation (8).

Equation (5) can then be approximated by:

$$\sigma_J(\lambda,t)\simeq w'(\lambda,t)+\frac{1}{\mu(t)}\left\{w'\left(\frac{\lambda}{\mu(t)},0\right)-w'\left(\frac{\lambda}{\mu(t)},1\right)\right\}+\frac{\eta_s}{\mu(t-\sqrt{t})}w'\left(\frac{\lambda}{\mu(t-\sqrt{t})},\sqrt{t}\right)\ln t \tag{11}$$

Now Bernstein and Zapas have shown that when the relation:

$$\int_{\lambda_1}^{\lambda_2}\sigma_J(\lambda,t)d\lambda-(\lambda_2-\lambda_1)\sigma_0=B \tag{12}$$

is positive ($B>0$) the bar will continue to elongate in a homogeneous fashion. In equation (12), σ_0 is the engineering stress that the material has at time t after a history $\mu(\tau)$. When B becomes zero, the bar reaches an insipient point of instability in which case small flaws or inhomogeneities in the specimen will cause it to neck. When B becomes negative (in *Figure 1* the condition that $A_2>A_1$) the material will find itself in multiple stages of elongation.

Equation (12) can be rewritten as:

$$\int_{\ln\lambda_1}^{\ln\lambda_2}\lambda\sigma_J(\lambda,t)d\ln\lambda-(\lambda_2-\lambda_1)\sigma_0=B \tag{13}$$

Consider now a constant rate of strain experiment, in particular our data shown in *Figure 4* for the situation

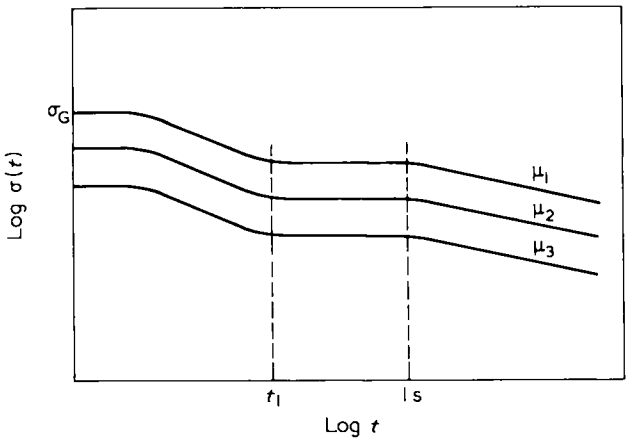

Figure 9 Log $\sigma(t)$ *versus* log t showing transition region

where the rate $\kappa = 6.0 \times 10^{-4}$ and $\mu(\tau) = 0.19$. Experimentally this was the point at which a neck started to appear. In *Figure 10* we have constructed the jump curve showing $\lambda\sigma(\lambda,t)$ *versus* $\ln\lambda$, where A_1 and A_2 are equal. We now wish to show that the instability theory of Bernstein and Zapas can predict the experimental observation that, within a certain range of κ, necking occurs at higher values of strain as κ decreases. In a constant rate of strain experiment, necking occurs after the stress maximum is reached. Thus at elongations greater than that at which the neck occurs the stress will continue to decrease for a time before the plateau value is reached. Consider two constant rate of strain experiments, one done at rate κ_1, and the other at rate κ_2 where $\kappa_1 > \kappa_2$. If ε_{N1} is the strain at which necking occurred for rate κ_1, and at time $t_1 = \varepsilon_{N1}/\kappa_1$, then we wish to determine whether the material will be stable when it reaches the same strain at rate κ_2 and time $t_2 = \varepsilon_{N1}/\kappa_2$. To a first approximation the ratio of the two Maxwell lines will be:

$$\frac{\sigma_{01}}{\sigma_{02}} \simeq \frac{w'(1+\varepsilon_{N_1}\varepsilon_{N_1}/\kappa_1)}{w'(1+\varepsilon_{N_1},\varepsilon_{N_1}/\kappa_2)} = R \tag{14}$$

where in *Figure 1* the Maxwell line is the horizontal line drawn at σ_0, or $(A_1 = A_2)$. With the condition that $\mu(t) = 1 + \varepsilon_{N_1}$, we rewrite equation (11) as:

$$9\sigma_{J_1}(\lambda,t_1) = w'(\lambda_1 t_1) + \frac{\eta_s}{\mu(t_1-\sqrt{t_1})} w'\left(\frac{\lambda}{\mu(t_1-\sqrt{t_1})},\sqrt{t_1}\right)\ln r_1 + g \tag{15}$$

where $g = \frac{1}{\mu(t)}\left\{w'\left(\frac{\lambda}{\mu(t)},0\right) - w'\left(\frac{\lambda}{\mu(t)},1\right)\right\}$ is the contribution from the 'glassy region', and here is taken to be independent of time. Similarly,

$$\sigma_J(\lambda,t_2) = w'(\lambda,t_2) + \frac{\eta_s}{\mu(t_2-\sqrt{t_2})} w'\left(\frac{\lambda}{\mu(t_2-\sqrt{t_2})},\sqrt{t_2}\right)\ln t_2 + g \tag{16}$$

If equations (15) and (16) are compared term by term, one can conclude that:

$$\frac{\sigma_{J1}(\lambda,t_1)}{\sigma_{J2}(\lambda,t_2)} < R, \text{ for } \lambda > \mu(t) \tag{17}$$

It follows, then, that:

$$\frac{1}{R}\int_{\lambda_0}^{\lambda_s} \sigma_{J1}(\hat{\lambda},t_1)\mathrm{d}\hat{\lambda} < \int_{\lambda_0}^{\lambda_s} \sigma_{J2}(\hat{\lambda},t_2)\mathrm{d}\hat{\lambda} \tag{18}$$

where $\lambda_0 = 1 + \varepsilon_{N1}$ and λ_s is any λ greater than λ_0. If the quantity $\sigma_{02}(\lambda_s - \lambda_0)$ is subtracted from both sides of the inequality in equation (18), then:

$$\frac{1}{R}\int_{\lambda_0}^{\lambda_s} \sigma_{J1}(\hat{\lambda},t_1)\mathrm{d}\hat{\lambda} - (\lambda_s-\lambda_0)\sigma_{02} < \int_{\lambda_0}^{\lambda_s} \sigma_{J2}(\hat{\lambda},t_2)\mathrm{d}\hat{\lambda} - (\lambda_s-\lambda_0)\sigma_{02} \tag{19}$$

From equation (14), $\sigma_{02} = \sigma_{01}/R$; so that:

$$\frac{1}{R}\left\{\int_{\lambda_0}^{\lambda_s} \sigma_{J1}(\hat{\lambda},t_1)\mathrm{d}\hat{\lambda} - (\lambda_s-\lambda_0)\sigma_{01}\right\} < \int_{\lambda_0}^{\lambda_s} \sigma_{J2}(\hat{\lambda},t_2)\mathrm{d}\hat{\lambda} - (\lambda_s-\lambda_0)\sigma_{02} \tag{20}$$

But the quantity inside the brackets on the left hand side of the equation is zero since σ_{01} has been taken as the stress at the insipient point of instability. Therefore:

$$\int_{\lambda_0}^{\lambda_s} \sigma_{J2}(\hat{\lambda},t_2)\mathrm{d}\hat{\lambda} - (\lambda_s-\lambda_0)\sigma_{02} > 0 \tag{21}$$

Thus in a constant rate of strain experiment carried out at a lower rate of strain than the value κ_1 the point of instability will occur at a larger strain. This result is in agreement with our experimental observations as is shown in *Figure 4*. By a similar argument this same result can be shown to be true for other strain histories which we have examined, for example constant rate of stress and creep. In *Figure 5* it can be seen that the strain at which necking occurs becomes larger as the rate of loading decreases. In the creep experiment (*Figure 8*) the line α

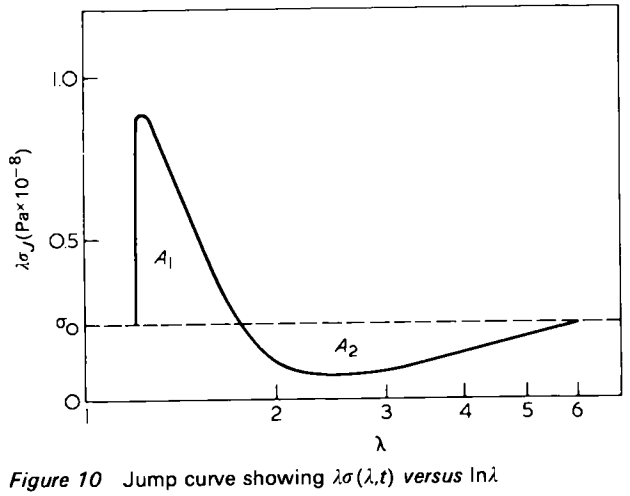

Figure 10 Jump curve showing $\lambda\sigma(\lambda,t)$ *versus* $\ln\lambda$

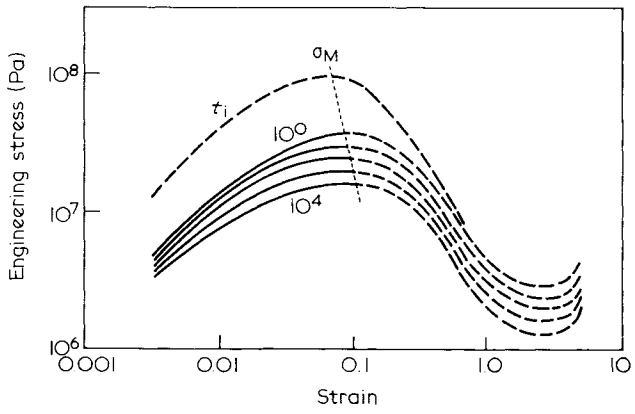

Figure 11 Log $w'(\lambda,t)$ *versus* $\log(\lambda-1)$

corresponding to necking shifts to larger strains as the load decreases.

For a quantitative description of the point at which the instability occurs one needs isochronal data over a much wider range of strains than can be obtained from single step stress–relaxation experiments. In the present work we have constructed one possible set of isochrones by extrapolating our data into the region of very high strains. This particular surface cannot, by any means, be considered unique. It is designed to be in agreement with the available experimental results. From the constant rate of strain experiments, and using the BKZ theory, it can be deduced that each isochrone should go through a maximum at a strain very close to the point where the maximum stress occurs in a constant rate of strain experiment. Experiments also show that the maxima are shifted to smaller strains at shorter times. This behaviour indicates that the assumption made earlier in deriving equation (10) is not strictly true. The assumption that on a double logarithmic plot the isochrones were parallel was made in order to give a simple example. From stress–relaxation data obtained on a specimen which had been elongated and then allowed to relax to a value of λ as high as 9.5, it was found that at the very early times the stress levelled off to a value which yielded a modulus higher than that corresponding to the instantaneous modulus of the undrawn material. Also, at times greater than about 5 s the stress shows a time dependence and a rate of decay that is comparable to that of the undrawn material. Therefore, we shall assume that in the region of very large strain the isochrone for time $t=0$ is the same as that for $t=1$. It is also assumed that at strains greater than about 10% the rate of relaxation is independent of the level of strain. This assumption appears to be reasonable based on data which we have obtained on a sample of very high molecular weight linear polyethylene ($M_w \simeq 4\times10^6$). In the case of this polyethylene, which does not exhibit necking, we have been able to obtain stress relaxation data at very high extensions, and the logarithm of the rate of relaxation was found to be independent of the level of strain. Finally from creep data we know that the necked polypropylene has a 'natural draw' of about $\lambda=6$, as is indicated by the line β in *Figure 8*.

From the Bernstein and Zapas theory it is known that following the occurrence of the maximum in the isochrones there must be a minimum before the natural draw is reached. On the assumption that the isochrones must be smooth, and using all of the available experimental results just described, we have constructed, by trial and error, the diagram shown in *Figure 11*. For ease of construction we have plotted it in terms of log $w'(\lambda,t)$ *versus* log $(\lambda-1)$. Assuming that the dotted line in *Figure 11* connects all the maxima, we can deduce the position of the maximum for the isochrone due to the instantaneous modulus ($t=0$). From the surface shown in *Figure 11* we have calculated the behaviour for several constant rate of strain and creep experiments and the calculated values for the point of instability are well within the experimental reproducibility. This result should not be surprising since the same experimental results were used in constructing the surface. We have also calculated the point of instability for the two step constant rate of loading experiment described in *Figure 5* and the calculated value was found to be the same as that observed experimentally.

CONCLUSION

We can say that the Bernstein and Zapas instability theory may provide a reasonable description of the phenomenon of necking, and with the aid of experiments involving a variety of different strain histories one can construct a surface of isochrones of stress *versus* strain from which it is possible to predict the point at which necking will occur for other strain histories. This, we believe, may turn out to be a valuable procedure for predicting the insipient point of necking for even more complicated strain histories. The present work should be considered only as a first step for further investigation into the understanding of the phenomena of instabilities which may occur in other polymers.

REFERENCES

1 Ericksen, J. L. *J. Elast.* 1975, **5**, 191
2 Bernstein, B. and Zapas, L. J. *J. Rheol.* 1981, **25**, 83
3 Bernstein, B., Kearsley, E. A. and Zapas, L. J. *Trans. Soc. Rheol.* 1963, **7**, 391
4 Passaglia, E. and Martin, G. M. *J. Res. NBS* 1964, **68A**, 519
5 Crissman, J. M. *J. Polym. Sci.* A-2 1969, **7**, 389
6 American Society for Testing and Materials 1965 Book of ASTM Standards, Part 28. (This test method is no longer included in the annual book of ASTM Standards.)
7 American Society for Testing and Materials 1976 Annual Book of ASTM Standards, Part 35
8 Zapas, L. J. and Phillips, J. C. *J. Res. NBS* 1971, **75A**, 33
9 Crissman, J. M. and Zapas, L. J. *Polym. Eng. Sci.* 1979, **19**, 99
10 Zapas, L. J. and Crissman, J. M. ACS Symposium Series, No. 95, Durability of Macromolecular Materials, (Ed. R. K. Eby), 1978, p. 301